

# HMM BASED ANOMALOUS SIGNAL DETECTION FROM ELF ELECTROMAGNETIC WAVE SIGNALS

Yoshinao Ito<sup>†</sup>, Akitoshi Itai<sup>††</sup>, Hiroshi Yasukawa<sup>†††</sup>, Ichi Takumi<sup>‡</sup> and Masayasu Hata<sup>‡‡</sup>

<sup>†,††,†††</sup>Aichi Prefectural University, Nagakute, Aichi 480-1198, Japan

E-mail: <sup>†</sup>im092002@cis.aichi-pu.ac.jp, <sup>††</sup>a.itai@cis.aichi-pu.ac.jp, <sup>†††</sup>yasukawa@ist.aichi-pu.ac.jp

<sup>‡</sup>Nagoya Institute of Technology, Showa-ku, Nagoya 466-8555, Japan

E-mail: takumi@ics.nitech.ac.jp

<sup>‡‡</sup>Chubu University, Kasugai-shi, 487-8501 Japan

E-mail: hata@cs.chubu.ac.jp

## ABSTRACT

It is known that the detection of a seismic radiation emitted from the earth's crust is useful for predicting earthquakes. We have been observing the electromagnetic (EM) wave in the Extremely Low Frequency (ELF) band. Various methods have been proposed to detect an anomalous EM radiation from recorded data. In this paper, we propose the anomalous signal detection based on HMM whose input vector is the amplitude density distribution of an EM wave. The amplitude density distribution is calculated from the image of an EM wave data. The optimal scale of an image to calculate an amplitude density distribution is examined with use of a false detection rate. Moreover the optimal number of states of HMM is investigated to achieve an accurate detection.

## 1. INTRODUCTION

Anomalous radiation of EM waves due to an earth diastrophism has been recorded in advance of earthquakes and volcanic activities[1]. We have been measuring the EM radiation in the ELF band. Our research is directed towards identifying an anomalous radiation of earthquakes from the EM wave data[2]. Observed signals contain undesired components associated with the magnetosphere, the ionized layer and the lightning radiation in the tropics, and so on[3]. Various signal processing techniques have been proposed to detect and understand the anomalous radiation in the ELF band.

The normal value method[4] and the principal component analysis[5] were proposed as simple and reasonable anomalous signal detection. These methods require the observation signal recorded over several years at the same observation point. Due to this limitation, it is difficult to detect an anomalous signal in a new observation point. The neural network[6] was applied to overcome the weakness of conventional methods. The observation signal at the same point is not necessary for the training of the neural network. However, in order to achieve the accurate detection, many anomalous signals related to the great earthquake are necessary as the training data set. The anomalous signal detection using a linear prediction error detects a seismic signal without anomalous signals. However, abrupt noises are detected as an anomalous signal.

Requirements for an anomalous signal detection are outlined below.

- An anomalous signal can be detected at a different observation point.
- Decrease the number of anomalous signal as training data

- Decrease the false detection due to an abrupt noise

In this paper, the HMM is applied as the anomalous signal detection satisfying the above requirements. The HMM input signal the amplitude density distribution calculated from the waveform of the EM wave data excluding the anomalous signal. The training data is observed at various seasons and observation points. The observation signal including the abrupt noise is also used as training data to avoid the false detection. Results of the anomalous signal detection will indicate the different characteristics when the display scale of the waveform is changed. The number of states of HMM influence the anomalous signal detection accuracy. This paper represents the optimal display scale of the image and the number of state of HMM.

## 2. ELECTROMAGNETIC WAVE

We observed the EM wave radiation in the ELF band (223Hz) as represented by the east-west, north-south, and vertical magnetic field components at about forty observation stations in Japan (Fig.1). Collected data is averaged over 6 seconds interval (14400 points per day) at each station and direction. The EM wave data averaged over 6 and 150 seconds interval is recorded on the data logger established in Nagoya Institute of Technology. The data server provides us the numerical data and its graphical image. The typical seismic radiation from the earth's crust observed in the ELF band has a field strength of about on pico tesla normalized by the square root of one frequency ( $\text{pT}/\sqrt{\text{Hz}}$ ).

A signal observed at Aomori-Hachinohe station is shown in Fig.2. The vertical axis represents a density of a magnetic flux ( $\text{pT}/\sqrt{\text{Hz}}$ ), the horizontal axis indicates the time. The right-hand side origin is set to 0:00 AM, August 13th, 2001. An earthquake occurred on the 13th of August 2001.

The seismic radiation must be extracted accurately, from the observation signal including various noises, due to a sensor noise, an artificial noise, a noise from atmosphere and magnetosphere. The observed EM wave data in ELF band consists of three components given below.

- **Background noise:** The dominant background noise is the lightning radiation from the tropics. It passes between the ionized layer and the surface of the earth. It is weak in the daytime and strong at night because of the properties of propagation path. Furthermore, it has a seasonal trend from about 1 to 2  $\text{pT}/\sqrt{\text{Hz}}$  in summer to 0.3 to 1  $\text{pT}/\sqrt{\text{Hz}}$  in winter.

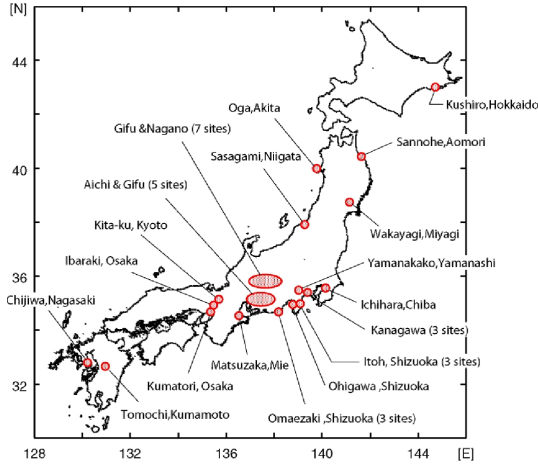


Figure 1: Observation sites for ELF EM wave measuring in ELF band

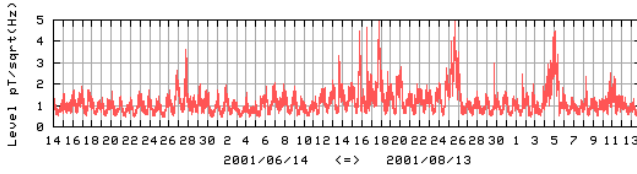


Figure 2: Observed EM wave

- **Anomalous signal:** The typical anomalous signal is recorded a level from 0.1 to tens of  $\text{pT}/\sqrt{\text{Hz}}$ , and is dependent on the scale of the earthquake event, its depth and a distance to the observation point.
- **Abrupt noise:** Spike noises are common and significantly degrade the accuracy of detecting the anomalous signal. The main cause is the incomplete removal of a sensor noise and the effect of a thunder radiation in near field. These spikes are short and have strong amplitude from several  $\text{pT}/\sqrt{\text{Hz}}$  to several tens  $\text{pT}/\sqrt{\text{Hz}}$ .

Assume that EM wave data at time  $t$  is  $x(t)$ , it is represented as the sum of a background noise component  $T(t)$ , an anomalous signal  $P(t)$  and other noises  $w(t)$ . A model of the observed data is expressed as;

$$x(t) = T(t) + P(t) + w(t). \quad (1)$$

Our goal is to detect the  $P(t)$  accurately. In this paper, observed data is divided into two categories. One includes the anomalous, another does not contain the  $P(t)$ . The former expressed as  $T(t) + P(t) + w(t)$  is called as an anomalous pattern, the latter represented by  $T(t) + w(t)$  is referred as a normal pattern.

### 3. HIDDEN MARKOV MODEL

#### 3.1 Configuration of HMM

In this paper, a HMM[7] is adopted to detect the anomalous signal from the EM wave data. The HMM with left-to-right type (Fig.3) is employed. The HMM has parameter states transition probability  $a_{ij}$  which consists of state  $q_i$ ,

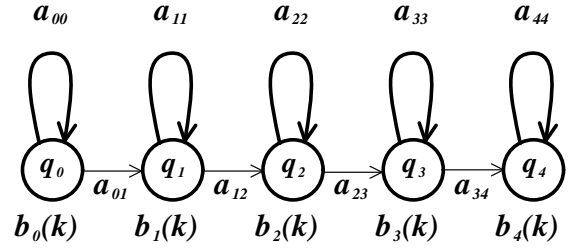


Figure 3: State transition diagram for a 5-state left-to-right HMM

state transition probability  $a_{ij}$  and observation symbol probability  $b_j(k)$ .

- **States:**  $q_0, q_1, q_2, \dots, q_{N-1}$   
HMM is composed by  $N$  states. Each state provides the state transition connected to a next state and itself.
- **State transition probability:**  $a_{ij}$   
 $a_{ij}$  is the transition probability of transitioning from a state  $q_i$  to a state  $q_j$ .  $a_{ij}$  satisfies  $0 \leq a_{ij} \leq 1$  with

$$\sum_j a_{ij} = 1. \quad (2)$$

- **Observation symbol probability:**  $b_j(k)$   
Observation symbol probability in a state  $q_j$  is expressed as  $b_j(k)$ , where  $k$  is the observation symbol.  $b_j(k)$  satisfies;

$$\sum_k b_j(k) = 1. \quad (3)$$

Each parameter is estimated by using Baum-Welch algorithm whose training data is composed by the normal pattern data. The trained HMM outputs a high-acceptance probability for a normal pattern, while a low-acceptance probability for an anomalous pattern.

#### 3.2 Baum-Welch Algorithm

In order to use the HMM for a pattern recognition, a parameter  $a_{ij}$  and  $b_j(k)$  should be estimated. The Baum-Welch algorithm based on EM algorithms is applied to calculate HMM parameters by using given symbols extracted from observation signals. The Baum-Welch algorithm is composed by the forward and backward algorithm.

- **Forward algorithm:** Assume that observed symbols are  $O = O_1 O_2 \dots O_T$ , states are  $Q = q_1 q_2 \dots q_T$ . The observation probability is calculated when the observed partial series  $O = O_1 O_2 \dots O_t$  is observed in state  $q_i$  at time  $t$ . The forward probability  $\alpha_t(i)$  is calculated as;

$$\alpha_t(i) = \sum_{j=0}^{N-1} \alpha_{t-1}(j) a_{ij} b_j(k_t) \quad (4)$$

where,  $k = k_0 k_1 \dots k_t \dots k_{T-1}$  is an observed symbol.

- **Backward algorithm:** The observation probability is calculated when the observed partial series  $O = O_{t+1} O_{t+2} \dots O_T$  is observed in state  $q_i$  at time  $t$ . The backward probability  $\beta_t(i)$  is calculated as;

$$\beta_t(i) = \sum_{j=0}^{N-1} \beta_{t+1}(j) a_{ij} b_j(k_{t+1}). \quad (5)$$

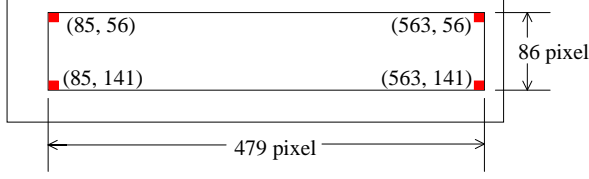


Figure 4: Waveform area in the image of EM wave data

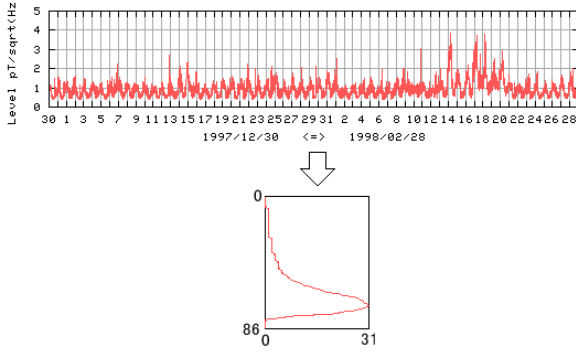


Figure 5: Observed signal and input symbols

### 3.3 Viterbi Algorithm

The acceptance probability of HMM is calculated by the Viterbi algorithm. The likelihood at the time  $t$  in the state  $q_i$  is expressed as;

$$\log(f(i, t)) = \max_j \log(f(j, t-1)) + \log(a_{ji}) + \log(b_j(k_t)). \quad (6)$$

The log likelihood  $f(N-1, T)$  of the final state  $q_{N-1}$  at time  $t = T$  is defined as the acceptance probability.

## 4. INPUT OF HMM

The observation symbol is defined as the amplitude density distribution calculated from EM wave data. The symbol is extracted from the waveform of an EM wave data provided by a data server. The procedure of a symbol extraction is given as following steps:

1. Acquire the Graphics Interchange Format (GIF) file of EM wave data
2. Convert GIF image into Microsoft Windows Bitmap Image (BMP) image
3. Extract the waveform area (Fig.4)
4. Count the number of pixels of waveform area at each line ( $o = o_1 o_2 \dots o_{86}$ )
5. Input symbol  $O = O_1 O_2 \dots O_{86}$  is calculated by a normalizing coefficient  $S$  and  $o$ , as shown in (7) and (8)

$$S = \frac{\max o}{31} \quad (7)$$

$$O = o \cdot S. \quad (8)$$

The input image and its observation symbol  $O$  is shown in Fig.5.

Table 1: Combination of training data and test data

| training data | test data |
|---------------|-----------|
| ABCD          | EF        |
| ABCE          | DF        |
| ABDE          | CF        |
| ACDE          | BF        |
| BCDE          | AF        |

## 5. SIMULATION METHOD

The waveform of the EM wave data can be displayed on the following conditions.

- **X-axis**(Observation days): 1, 2, 7, 14, 30, 60 [days]
- **Y-axis**(Upper of density of magnetic flux): 3, 5, 10, 20, 50, 100, 200 [ $\text{pT}/\sqrt{\text{Hz}}$ ]

Anomalous signals are often observed several weeks before an earthquake. These signals tend to decrease just before the earthquake. This fact indicates that it is difficult to detect the anomalous signal from the image of X-axis 1 and 2 days. The image displayed with the scale of 7, 14, 30 and 60 days is used to the observation symbol extraction. Most of normal pattern signals are observed as a level of  $5 \text{ pT}/\sqrt{\text{Hz}}$  or less. It is known that the EM wave radiation recorded in the level of  $10 \text{ pT}/\sqrt{\text{Hz}}$  or more is the anomalous signal from an empirical knowledge. Therefore, as for the maximum value of Y-axis,  $10 \text{ pT}/\sqrt{\text{Hz}}$  or more is unnecessary. The image displayed with 5 or  $10 \text{ pT}/\sqrt{\text{Hz}}$  is used.

Fifty normal pattern data and ten anomalous pattern data for each scale are prepared. Fifty normal pattern data are divided into five groups named as group A, B, C, D and E. Each group includes ten normal pattern data respectively. Ten anomalous pattern data are called group F. Selected four groups of normal patterns are applied to HMM as training data. A remaining group normal pattern and the group F are applied to the trained HMM as test data (Table 1).

The threshold to distinguish between the normal pattern and the anomalous pattern is the lowest acceptance probability which is calculated from the test normal patterns. Therefore, one HMM has one threshold. The false detection is defined as a percentage of the number of anomalous signal which yields larger acceptance probability than threshold. This process is calculated with all combinations of display scale of the image, and number of state is changing from 1 to 10.

An example of the Log likelihood derived by HMM is shown in Fig.6. X-axis and Y-axis of the waveform is 14 days and  $5 \text{ pT}/\sqrt{\text{Hz}}$  respectively. In Fig.6, the horizontal axis shows a number of states of HMM, vertical axis is an Log likelihood. The solid line and the short dotted line indicates the Log likelihood calculated by the normal pattern and the anomalous pattern, respectively. From Fig.6, the Log likelihood of one anomalous pattern is larger than the threshold when the number of states is one, two and from six to ten.

## 6. SIMULATION RESULT

The false detection rate with various image display scales and the number of states is shown in Table 2. The lowest false detection rate is produced by the image scale of 14

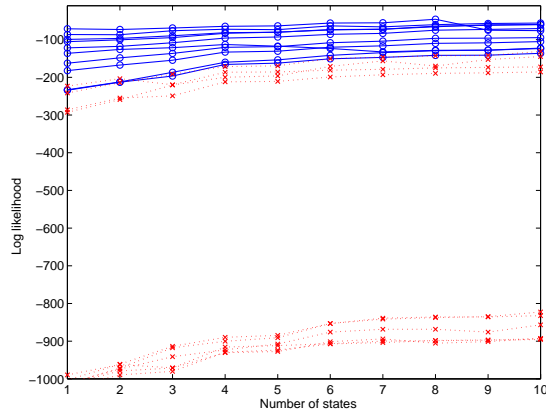


Figure 6: Example of false detection (Number of state vs. Log likelihood)

Table 2: False detection rate

| Scale of image |                           | False detection rate [%] |    |    |    |    |    |    |    |    |    |
|----------------|---------------------------|--------------------------|----|----|----|----|----|----|----|----|----|
| X-axis         | Y-axis                    | Number of state          |    |    |    |    |    |    |    |    |    |
| [days]         | [pT/ $\sqrt{\text{Hz}}$ ] | 1                        | 2  | 3  | 4  | 5  | 6  | 7  | 8  | 9  | 10 |
| 7              | 5                         | 10                       | 12 | 18 | 6  | 12 | 20 | 24 | 10 | 6  | 8  |
|                | 10                        | 12                       | 12 | 20 | 24 | 18 | 22 | 20 | 18 | 18 | 18 |
| 14             | 5                         | 0                        | 0  | 12 | 12 | 10 | 18 | 22 | 16 | 16 | 20 |
|                | 10                        | 8                        | 8  | 18 | 16 | 14 | 16 | 12 | 22 | 18 | 12 |
| 30             | 5                         | 12                       | 16 | 12 | 20 | 18 | 16 | 16 | 16 | 20 | 20 |
|                | 10                        | 14                       | 16 | 16 | 18 | 22 | 32 | 36 | 46 | 40 | 40 |
| 60             | 5                         | 10                       | 10 | 14 | 18 | 18 | 18 | 20 | 22 | 26 | 26 |
|                | 10                        | 14                       | 14 | 22 | 16 | 16 | 20 | 22 | 26 | 24 | 22 |

days,  $5\text{pT}/\sqrt{\text{Hz}}$ , and the number of states is one and two. Now we focus on the relationship between a display scale of Y-axis and a false detection. 29 false detection rates of the image displayed with  $5\text{pT}/\sqrt{\text{Hz}}$  are less than their  $10\text{pT}/\sqrt{\text{Hz}}$ . Therefore, the image displayed with  $5\text{pT}/\sqrt{\text{Hz}}$  is more effective to detect the anomalous signal than the image displayed with  $10\text{pT}/\sqrt{\text{Hz}}$ .

## 7. CONCLUSION

We proposed a HMM-based detection method of the anomalous signal related to EM wave radiated from earth's crust. The amplitude density distribution of the observed data calculated from the EM wave is adopted as the training data. The observation signal at various sites and seasons, and only normal pattern data is used as training data. It is shown that proposed method has a possibility of obtaining a good performance on the anomalous signal detection.

As future works, we consider the more good condition of HMM, about number of state and image display scale. And, the abrupt noise is evaluated by using the false detection.

## Acknowledgment

This research was supported in part by JSPS for the Grant-in-Aid for Scientific Research (A)20246068.

## REFERENCES

- [1] M.B.Gokhberg, V.A.Morgunov, T.Yoshio and I.Tomizawa: Experimental Measurements of Electromagnetic Emissions Possibly Relate to Earthquakes in Japan, *Journal of Geophysical Research*, 87, pp.7824-7829, 1982.
- [2] M.Hata, I.Takumi, S.Adachi and H.Yasukawa: An Analytical Method to Extract Precursor from Noisy Atmospherics, *Proc. of European Geophysical Society XXV*, NH014, pp.25-29, 2000.
- [3] M.Hata, I.Takumi and S.Yabashi: A Model of Earthquake Seen by Electromagnetic Observation - Gaseous Emission from the Earth as Main Source of Pre-Seismic Electromagnetic Precursor and Trigger of Followed Earthquake, *Proceedings of European Geophysical Society*, NH080, 1998.
- [4] S.Niwa, H.Yasukawa, M.Hata and I.Takumi: A Signal Detection on Precursor of Earthquake Using Normal Value for ELF Electromagnetic Wave Observation, *Proc. of Int. Sympo. on Information Theory and Its Applications*, pp.863-866, 2002.
- [5] S.Niwa, H.Yasukawa, M.Hata and I.Takumi: A Study on Precursor Signal Extraction with PCA for Predicting Significant Earthquakes, *IEICE Trans. Fund.*, Vol.E86-A, No.8, pp.2047-2052, 2003.
- [6] A.Itai, H.Yasukawa, I.Takumi and M.Hata: Anomalous Signal Detection Using Multi-layer Neural Network for Electromagnetic Wave Radiation, *Proc. of Int. Midwest Symposium on Circuits and Systems*, pp.III-259-262, Ohio, 2005.
- [7] Christoph M.Bishop: *Pattern Recognition and Machine Learning*, Springer, 2008.